Thickness dependence of superconductivity in single-crystal $Ta_4Pd_3Te_{16}$ nanoribbons

Lin Bao, Yiqing Bi, Xiaotong Liu, Xiaohui Yang, Tingting Hao, Shibing Tian, Zongli Wang, Junjie Li, and Changzhi Gu

Citation: Appl. Phys. Lett. **113**, 022603 (2018); doi: 10.1063/1.5040046
View online: https://doi.org/10.1063/1.5040046
View Table of Contents: http://aip.scitation.org/toc/apl/113/2
Published by the American Institute of Physics

Thickness dependence of superconductivity in single-crystal $Ta_4Pd_3Te_{16}$ nanoribbons

Lin Bao,[1] Yiqing Bi,[1] Xiaotong Liu,[1] Xiaohui Yang,[1] Tingting Hao,[2] Shibing Tian,[2] Zongli Wang,[1,a)] Junjie Li,[2,b)] and Changzhi Gu[2,c)]
[1]*Department of Physics, Zhejiang University, Hangzhou 310027, China*
[2]*Institute of Physics, Chinese Academy of Sciences, Beijing 100190, China*

(Received 14 May 2018; accepted 22 June 2018; published online 9 July 2018)

We present the thickness-dependent electrical properties of mechanically exfoliated single crystal $Ta_4Pd_3Te_{16}$ nanoribbons. By decreasing the nanoribbon thickness in the range of 500–20 nm, we observed a suppression of superconductivity driven by both the thickness and the external magnetic field. In particular, for the thinner nanoribbons with the thickness less than 40 nm, there is a non-zero resistance state extending down to low temperature, followed by the loss of superconductivity when the thickness is decreased to the order of the coherence length. We found that the theory of a thermally activated phase slip can well describe the temperature dependence of the resistance below T_c. The disorder-induced enhanced Coulomb interaction with the decrease in the thickness is expected to be dominant in the gradual crossover behavior from superconducting to normal or very weakly insulating behavior in the low-dimensional system. *Published by AIP Publishing.*
https://doi.org/10.1063/1.5040046

Superconductivity in low-dimensional systems has long attracted much attention due to their unconventional nature[1,2] and the simplicity of theoretical description.[3] Numerous studies have illustrated that the superconductivity can be successfully suppressed due to either disorder-induced localization of Cooper pairs,[4] weakening of Coulomb screening,[5] or generation and unbinding of vortex-antivortex pairs[6] by decreasing the size of low-dimensional systems. Furthermore, unlike in bulk superconductors, the resistance in low-dimensional superconductors gradually decreases below the onset temperature of superconducting transition (T_c) due to the thermally activated phase-slip (TAPS) and possible quantum phase-slip processes.[7–9] For example, in the extremely thin amorphous Bi films,[10] the thickness-dependent superconductor-insulator transition (SIT) can be attributed to the disorder, where the critical sheet resistance is almost equal to the quantum resistance $R_q = h/4e^2$. In comparison, in the rectangular shaped Nb_2PdS_5 nanowires with the size much larger than their phase coherence length,[11] a clear cross-sectional area dependent SIT with quasi-one-dimensional (quasi-1D) superconducting behavior is observed, and the temperature dependence of resistance below T_c can be described by the TAPS theory without any signature of quantum fluctuations. Therefore, it still remains to be fully understood what is the mechanism of driving the change in superconductivity as their size is reduced and how about the behavior of resistance below T_c in the low-dimensional superconductors.

The ternary telluride $Ta_4Pd_3Te_{16}$ crystal is a recently discovered layered superconductor with quasi-1D characteristics.[12,13] The superconducting transition occurs at about 4.5 K, and the coherence length is estimated to be about 15–21 nm along the *b*-axis.[14,15] Soon after this finding, the scanning tunnelling microscopy (STM),[15] thermal conductivity,[16] and Raman scattering[17] measurements have proposed several novel features in this multiband system, including the anisotropic gap structure, the existence of possible node, and charge-density-wave (CDW). Therefore, the $Ta_4Pd_3Te_{16}$ single crystals should be one of the extremely attractive candidates for studying the unconventional superconducting properties of low-dimensional systems.

In this work, we report the electrical transport measurements on exfoliated single-crystal $Ta_4Pd_3Te_{16}$ nanoribbons with different thicknesses. The results show that the superconductivity of $Ta_4Pd_3Te_{16}$ nanoribbons can be gradually suppressed by decreasing the thickness of nanoribbons, suggesting a direct and credible experimental evidence of the nature of thickness-dependent superconductivity in the layered quasi-1D compound $Ta_4Pd_3Te_{16}$. Such a gradual crossover behavior from superconducting to normal or very weakly insulating behavior can be also achieved by applying the external magnetic field. In addition, the temperature dependence of the resistance below T_c can be well explained by the TAPS theory.

The $Ta_4Pd_3Te_{16}$ crystals were grown using the self-flux method.[13] The flattened needle-like single crystals have the typical dimensions of about $2.5 \times 0.25 \times 0.1\ mm^3$. Because of the layered quasi-1D characteristics, $Ta_4Pd_3Te_{16}$ single crystals can be cleaved easily into rectangular shaped nanoribbons with different thicknesses. In our experiments, we used the Scotch tape method[18] to exfoliate $Ta_4Pd_3Te_{16}$ from as-grown bulk crystals onto a Si substrate covered with 300 nm SiO_2, in which the $Ta_4Pd_3Te_{16}$ nanoribbons with widths ranging from 200 nm to 1 μm and lengths from 10 μm to 50 μm were collected.

Figure 1(a) shows a scanning electron microscopy (SEM) image of a typical $Ta_4Pd_3Te_{16}$ nanoribbon with a thickness of about 150 nm, which is of uniform width. To examine the quality of the exfoliated nanoribbons, we used transmission electron microscopy (TEM) to observe the high-resolution TEM image and electron diffraction pattern as shown in

a)Electronic mail: zlwang@zju.edu.cn
b)Electronic mail: jjli@iphy.ac.cn
c)Electronic mail: czgu@iphy.ac.cn

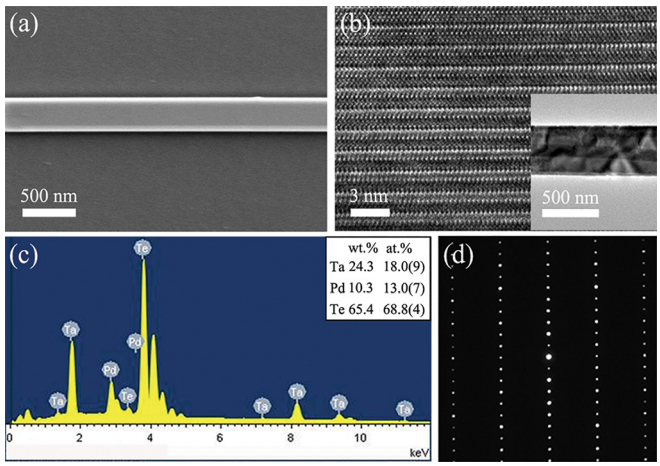

FIG. 1. (a) SEM image of a typical $Ta_4Pd_3Te_{16}$ nanoribbon obtained by mechanical exfoliation. (b) High-resolution TEM image of a randomly selected nanoribbon (inset of the panel). (c) and (d) The energy dispersive X-ray spectra and the electron diffraction pattern of the nanoribbon.

Figs. 1(b) and 1(d), respectively. It is obvious that the exfoliated nanoribbon is of a well-resolved chainlike structure along the *b*-axis and single crystal nature without any granular-like structure. In addition, the nanoribbons are relatively stable in the air with an oxidation layer of about 2–3 nm on the surface (no shown here). The thickness and width of nanoribbons were measured using atomic force microscopy (AFM). The chemical composition was determined by energy dispersive X-ray spectroscopy analysis (EDX), and the atomic ratio of Ta:Pd:Te is 4:3:16 within the measurement precision (±3%–5% depending on the elements measured), as shown in Fig. 1(c), in agreement with the expected value.

To assess the electronic properties of $Ta_4Pd_3Te_{16}$ nanoribbons, the contact electrodes were patterned on the nanoribbons using standard ultraviolet lithography followed by electron beam evaporation of Ti/Au (10/100 nm) in sequence. Then, the transport measurements were carried out from room temperature to 2 K with a Quantum Design Physical Properties Measurement System (PPMS) equipped with a 9 T superconducting magnet. The resistance of each sample was obtained by a standard four-terminal configuration with the driving current of 0.5–1 μA flowing along the *b*-axis and the magnetic fields aligned parallel to the *c*-axis of the nanoribbon.

Figures 2(a) and 2(b) show the temperature dependence of resistance for the typical superconducting sample S1 and non-superconducting sample S8, respectively. With the temperature cooling from room temperature to about 10 K, all the *R*–*T* curves show a positive slope ($dR/dT > 0$), indicating a metallic characteristic. Moreover, the fitting results about these $R(T)$ data reveal that they almost obey $R = R_0 + AT^2$ from 35 K to 5 K, as shown in the inset of Fig. 2(a). It is one of the features of Fermi liquid, consistent with that reported from the bulk crystal.[13] When the temperature is below 5 K, the *R*–*T* curves show a strong thickness-dependent feature, as clearly shown in Fig. 2(c). For the thickest nanoribbon S1 (500 nm), a superconducting transition takes place with the T_c of about 4.1 K. When the thickness of the nanoribbon is decreased to about sub-20 nm which is close to the estimated coherence length,[14,15] the superconducting transition disappears completely, signifying a normal or very weakly

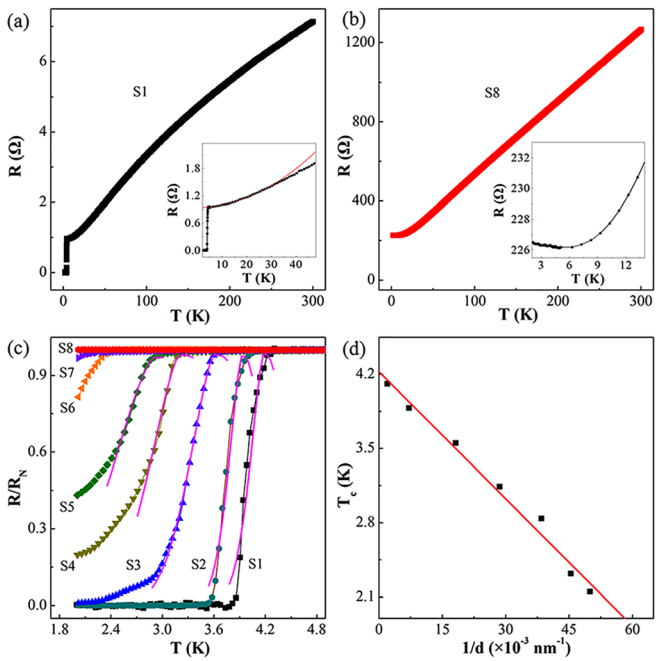

FIG. 2. Thickness-dependent superconductivity of the $Ta_4Pd_3Te_{16}$ nanoribbons at zero magnetic field. (a) and (b) The *R*–*T* curves for the nanoribbons of S1 and S8. The corresponding inset shows the expanded view of the low-T data confirming the resistive signature of the Fermi liquid for sample S1 and very weakly insulating behavior for sample S8, respectively. (c) Low-T parts of the normalized resistance (R/R_N) versus temperature for various samples with different thicknesses. R_N is the normal state resistance at 5 K, and the thicknesses are about 500, 140, 55, 35, 26, 22, 20, and 18 nm for sample S1–S8, respectively. The red solid lines are the fitting to the theory of thermally activated phase slips with the following fitting parameters. Transition temperatures are $T_c = 4.1$, 3.9, 3.6, 3.2, and 2.9 K. Coherence lengths are $\xi(0) = 5.2$, 13.0, 11.6, 18.6, and 22.7 nm. (d) T_c as a function of $1/d$ for various superconducting samples. The solid line is the fitting to a linear empirical relation.

insulating behavior [the inset of Fig. 2(b)]. For clarity, T_c versus the inverse of the nanoribbon thickness ($1/d$) is plotted in Fig. 2(d) for the superconducting samples. It is obvious that there is a linear empirical relation between T_c and $1/d$, as observed in 2D films.[19,20] Then, we can easily deduce that in the limit of $d \to \infty$, $T_c = 4.2$ K, which is very close to the measured in bulk crystals. Here, we noted that the width of the nanoribbon is much larger than its phase coherence length. Therefore, these results indicate that the crucial parameter in driving the suppression of superconducting transition may be the thickness rather than the cross sectional area of the nanoribbons.

From Fig. 2(c), we also noticed that with the decrease in T_c, the corresponding superconducting transition width is broadened followed by the appearance of a non-zero resistance state for the thinner nanoribbons. For the thicker nanoribbons S1 and S2 whose thicknesses are larger than 100 nm, the evolution of resistance below T_c is very quick. For the nanoribbon of about 55 nm thickness, the transition below T_c first remains relatively narrow and then becomes wide. However, when the thickness is decreased to be less than 40 nm, the superconducting transition below T_c is further broadened and remains a non-zero resistance state. Note that the superconducting transition is suppressed gradually as the thickness decreases, which is different from the sharp transition in the bulk crystal. Here, the transition below T_c can be

attributed to TAPS processes,[7,11] which was formalized by Langer and Ambegaokar and reexamined by McCumber and Halperin (LAMH).[21,22] Such processes have been depicted to be

$$R_{LAMH} = \frac{\pi\hbar^2\Omega}{2e^2kT} e^{-\Delta F/kT}, \quad (1)$$

where $\Omega = (L/\xi)(\Delta F/kT)^{1/2}(1/\tau_{GL})$ is the attempt frequency, $\Delta F = \left(8\sqrt{2}/3\right)(H_c^2/8\pi)A\xi$ is the free energy barrier for phase slips, $\tau_{GL} = \pi\hbar/8k(T_c - T)$ is the Ginzburg Landau relaxation time, and $\xi(T) = \xi(0)(1 - T/T_c)^{-1/2}$ is the coherence length. L, H_c, and A are the length, the thermodynamic critical field, and the cross-sectional area, respectively. The theoretical fits based on the formulations to account for TAPS are shown in Fig. 2(c) as the red solid lines. Here, the extracted coherence length is basically consistent with the reported experimental results and gradually increases with the decrease in thickness, which should be due to the suppression of T_c partially. The agreement between the data and the model of phase slips strongly suggests that the TAPS theory can well describe the temperature dependence of the resistance below T_c for the $Ta_4Pd_3Te_{16}$ nanoribbons.

Then, we investigated the influence of the external magnetic field on superconducting transition for the superconducting nanoribbons with different thicknesses. Figures 3(a) and 3(b) show the temperature dependence of resistance at various magnetic fields for two representative superconducting samples S2 and S4, respectively. With the applied magnetic field increasing, T_c shifts to a lower value and the superconducting transition width increases. Here, the behavior of the magnetic field-induced superconducting transition is qualitatively similar to that driven by the reduction in the thickness as shown in Fig. 2(c), which suggests that the suppression of superconductivity in both cases has the same physical origin in the $Ta_4Pd_3Te_{16}$ nanoribbons.[23] On the other hand, we noticed that the superconductivity in thinner sample S4 is suppressed more dramatically than that in thicker sample S2. To clarify this phenomenon, the upper critical magnetic fields were acquired through the classical criterion of $R/R_N = 90\%$, where R_N is the normal state resistance at 5 K. The extracted H_{c2} of several nanoribbons with different thicknesses is shown in Fig. 3(c). Then, we used the linear extrapolations rather than the Werthamer-Helfand-Hohenberg (WHH) theory[24] to estimate the corresponding T = 0 upper critical magnetic fields [$H_{c2}(0)$]. We can see that $H_{c2}(0)$ decreases from about 2.6 T to 1.7 T with the thickness decreasing from 500 nm to 35 nm. Furthermore, in a series of nanoribbons with the thickness ranging from about 180 nm to 40 nm, $H_{c2}(0)$ almost decreases monotonically with the thickness decreasing, as shown in Fig. 3(d). In a word, the $H_{c2}(0)$ of $Ta_4Pd_3Te_{16}$ nanoribbons can be restrained by the reduction in the thickness, which might be partially due to the suppression of T_c.

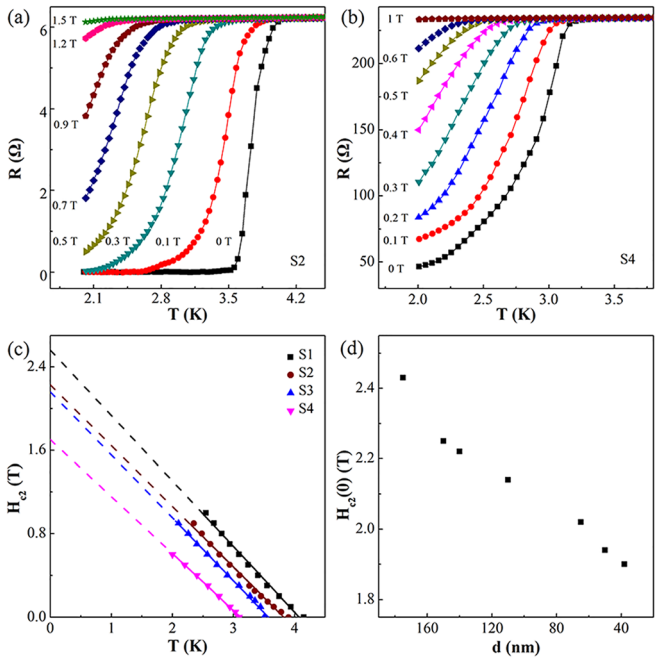

FIG. 3. (a) and (b) The *R*–*T* curves of the nanoribbons S2 and S4 at different magnetic fields, respectively. (c) The H_{c2}–T phase diagrams of several superconducting samples (S1, S2, S3, and S4), where the solid lines are the linear fits to the data and the dashed lines are the extension of the linear fitting to $H_{c2}(0)$. (d) $H_{c2}(0)$ versus d for series of superconducting samples with the thicknesses ranging from 180 nm to 40 nm.

Now, we turn to the physical origin of the observed crossover behavior from superconducting to normal or very weakly insulating behavior. First, we note that the normal state resistance at the transition point is much smaller than the quantum resistance $R_q \sim 6.45\,k\Omega$ and the thickness of the $Ta_4Pd_3Te_{16}$ nanoribbon is larger than its phase coherence length, excluding the possibility of quantum fluctuations.[25,26] Second, it is well-known that in the 1D limit, the disorder-induced Coulomb repulsion of electrons will be enhanced with the thickness decreasing, which can localize the electronic states and preclude the formation of Cooper pairing.[4,27] Hence, the superconductivity will be suppressed resulting from the depression of the magnitude of the order parameter by the enhanced Coulomb repulsion. The theories also predict that $\Delta T_c = T_c - T_{c0}$ is linear with $1/d$, and eventually, superconductivity is destroyed as T_c drops continuously to zero from the bulk value T_{c0}.[28] We found that our experimental results are consistent with such a linear behavior, as shown in Fig. 2(d). In addition, as observed in single crystal Sb_2Te_3 nanoflakes,[29] the increasing disorder in the superconducting nanoribbons with thickness decreasing can be elucidated by the decreasing slope of normalized resistance $R(T)/R_{300}$ (no shown here), where R_{300} is the resistance at 300 K. Therefore, we can conclude that the increasing disorder with the reduction in the nanoribbon thickness may play a crucial role in the suppression of superconducting transition in the quasi-1D compound. In our study, however, the accompanying non-zero resistance state is of a metallic state or a very weak insulating state rather than a clear insulating state as observed in Nb_2PdS_5 nanowires,[11] which suggests that the degree of disorder may be not enough to cause a clear SIT in the quasi-1D $Ta_4Pd_3Te_{16}$ nanoribbons. Note that for this purpose, an alternative experiment about the influence of Ga^+ irradiation on the properties of $Ta_4Pd_3Te_{16}$ nanoribbons has been carried out. The measurement results indicate that a clear insulating behavior or SIT could occur in the superconducting nanoribbon due to the increase in disorder by the Ga^+ irradiation, which is not the main content here and will be published elsewhere.

On the other hand, because the $Ta_4Pd_3Te_{16}$ crystal is stacked of many quasi-1D chains coupled to each other, the enhanced disorder-induced Coulomb repulsion competes with the interchain coupling in the chain with the thickness decreasing. As a result, T_c decreases gradually and then the non-zero resistance state appears, accompanying the loss of superconductivity at last when the thickness is decreased from about 500 nm to sub-20 nm that is close to the order of the coherence length. Similarly, the suppression of superconductivity by the applied magnetic field can be also qualitatively understood by the above-mentioned scenario. When the external magnetic field penetrates the nanoribbon, the interchain Josephson-like coupling can be suppressed and the Coulomb interaction in the chains will be dominant in the suppression of the amplitude of the order parameter, leading to the suppression of superconductivity in the quasi-1D compound $Ta_4Pd_3Te_{16}$.

In summary, the transport properties of single crystal $Ta_4Pd_3Te_{16}$ nanoribbons with different thicknesses have been investigated. The nanoribbons exhibit a clear thickness-dependent suppression of superconductivity when the nanoribbon thickness is decreased from about 500 nm to sub-20 nm. We found that the temperature dependence of the resistance below T_c can be explained by the TAPS theory, and the gradual crossover behavior from superconducting to normal or very weakly insulating behavior can be mainly attributed to the enhanced Coulomb interactions induced by the moderate increase in disorder with the reduction in the nanoribbon thickness. Furthermore, the preliminary experimental results from the Ga^+ irradiated $Ta_4Pd_3Te_{16}$ nanoribbons suggest that it is quite necessary to understand the nature of SIT in the $Ta_4Pd_3Te_{16}$ nanoribbons with a chainlike structure by inquiring into the effect of the degree of disorder in the following work.

We acknowledge helpful discussions with Professor MingLiang Tian. This work was supported by the National Basic Research Program of China (Grant No. 2014CB921201), the National Natural Science Foundation of China (Grant Nos. 61390503, 11574266, 11574385, and 11574369), the Strategic Priority Research Program of CAS (Grant No. XDB07020200), the Key Research Program of Frontier Sciences, CAS (Grant No. QYZDJ-SSW-SLH042), and the Fundamental Research Funds for the Central Universities (Grant No. 2017QNA3008).

[1]A. K. Geim, I. V. Grigorieva, S. V. Dubonos, J. G. S. Lok, J. C. Maan, A. E. Filippov, and F. M. Peeters, Nature **390**, 259 (1997).
[2]A. K. Geim, S. V. Dubonos, J. G. S. Lok, M. Henini, and J. C. Maan, Nature **396**, 144 (1998).
[3]H. C. Fu, A. Seidel, J. Clarke, and D. H. Lee, Phys. Rev. Lett. **96**, 157005 (2006).
[4]Y. Oreg and A. M. Finkel'stein, Phys. Rev. Lett. **83**, 191 (1999).
[5]J. M. Graybeal and M. R. Beasley, Phys. Rev. B **29**, 4167 (1984).
[6]W. W. Zhao, Q. Y. Wang, M. H. Liu, W. H. Zhang, Y. L. Wang, M. Chen, Y. Guo, K. He, X. Chen, Y. Y. Wang, J. Wang, X. C. Xie, Q. Niu, L. L. Wang, X. C. Ma, J. K. Jain, M. H. W. Chan, and Q. K. Xue, Solid State Commun. **165**, 59 (2013).
[7]C. N. Lau, N. Markovic, M. Bockrath, A. Bezryadin, and M. Tinkham, Phys. Rev. Lett. **87**, 217003 (2001).
[8]A. Rogachev and A. Bezryadin, Appl. Phys. Lett. **83**, 512 (2003).
[9]A. Rogachev, A. T. Bollinger, and A. Bezryadin, Phys. Rev. Lett. **94**, 017004 (2005).
[10]D. B. Haviland, Y. Liu, and A. M. Goldman, Phys. Rev. Lett. **62**, 2180 (1989).
[11]W. Ning, H. Y. Yu, Y. Q. Liu, Y. Y. Han, N. Wang, J. Y. Yang, H. F. Du, C. J. Zhang, Z. Q. Mao, Y. Liu, M. L. Tian, and Y. H. Zhang, Nano Lett. **15**, 869 (2015).
[12]A. Mar and J. A. Ibers, J. Chem. Soc., Dalton Trans. **0**, 639 (1991).
[13]W. H. Jiao, Z. T. Tang, Y. L. Sun, Y. Liu, Q. Tao, C. M. Feng, Y. W. Zeng, Z. A. Xu, and G. H. Cao, J. Am. Chem. Soc. **136**, 1284 (2014).
[14]W. H. Jiao, Y. Liu, Y. K. Li, X. F. Xu, J. K. Bao, C. M. Feng, S. Y. Li, Z. A. Xu, and G. H. Cao, J. Phys.: Condens. Matter **27**, 325701 (2015).
[15]Z. Y. Du, D. L. Fang, Z. Y. Wang, Y. F. Li, G. Du, H. Yang, X. Y. Zhu, and H. H. Wen, Sci. Rep. **5**, 9408 (2015).
[16]J. Pan, W. H. Jiao, X. C. Hong, Z. Zhang, L. P. He, P. L. Cai, J. Zhang, G. H. Cao, and S. Y. Li, Phys. Rev. B **92**, 180505(R) (2015).
[17]D. Chen, P. Richard, Z. D. Song, W. L. Zhang, S. F. Wu, W. H. Jiao, Z. Fang, G. H. Cao, and H. Ding, J. Phys.: Condens. Matter **27**, 495701 (2015).
[18]K. S. Novoselov, A. K. Geim, S. V. Morozov, D. Jiang, Y. Zhang, S. V. Dubonos, I. V. Grigorieva, and A. A. Firsov, Science **306**, 666 (2004).
[19]W. H. Tang, C. Y. Ng, C. Y. Yau, and J. Gao, Supercond. Sci. Technol. **13**, 580 (2000).
[20]E. Khestanova, J. Birkbeck, M. Zhu, Y. Cao, G. L. Yu, D. Ghazaryan, J. Yin, H. Berger, L. Forró, T. Taniguchi, K. Watanabe, R. V. Gorbachev, A. Mishchenko, A. K. Geim, and I. V. Grigorieva, Nano Lett. **18**, 2623 (2018).
[21]J. S. Langer and V. Ambegaokar, Phys. Rev. **164**, 498 (1967).
[22]D. E. McCumber and B. I. Halperin, Phys. Rev. B **1**, 1054 (1970).
[23]H. Kim, S. Jamali, and A. Rogachev, Phys. Rev. Lett. **109**, 027002 (2012).
[24]X. F. Xu, W. H. Jiao, N. Zhou, Y. Guo, Y. K. Li, J. H. Dai, Z. Q. Lin, Y. J. Liu, Z. W. Zhu, X. Lu, H. Q. Yuan, and G. H. Cao, J. Phys.: Condens. Matter **27**, 335701 (2015).
[25]M. P. A. Fisher, Phys. Rev. Lett. **65**, 923 (1990).
[26]P. Orgiani, C. Aruta, G. Balestrino, D. Born, L. Maritato, P. G. Medaglia, D. Stornaiuolo, F. Tafuri, and A. Tebano, Phys. Rev. Lett. **98**, 036401 (2007).
[27]B. L. Altshuler and A. G. Aronov, Phys. Rev. Lett. **44**, 1288 (1980).
[28]H. M. Jaeger, D. B. Haviland, B. G. Orr, and A. M. Goldman, Phys. Rev. B **40**, 182 (1989).
[29]W. H. Tsai, C. H. Chien, P. C. Lee, M. N. Ou, S. R. Harutyunyan, and Y. Y. Chen, e-print arXiv:1608.05337.